Supporting Information

Olsen et al. 10.1073/pnas.0911811107

SI Materials and Methods

Bacterial Strains and Construction of Isogenic MTSR Deletion Mutant and Complemented Strains. Strain MGAS315 (ATCC-BAA595) was cultured from a patient with streptococcal toxic shock syndrome. Strain MGAS9887, a clinical isolate with a naturally occurring truncation mutation in the *mtsR* gene, was collected in accordance with a protocol approved by the Institutional Review Board, Human Subjects Review Committee of the University of Toronto. The genome sequence of strain MGAS315 has been reported, and strain MGAS9887 has been characterized by comparative genome sequencing (1–3). Based on extensive phylogenetic analysis of ~350 serotype M3 GAS isolates collected during our ongoing prospective population-based molecular epidemiology study of invasive infections in Ontario that includes whole genome sequencing, genome resequencing of 95 serotype M3 strains, phage typing, and whole genome SNP typing, strains MGAS9887 and MGAS315 have been determined to be genetically representative of clinical isolates with the mutant and wild-type *mtsR* allele, respectively (1–3). That is, strains MGAS9887 and MGAS315 possess all genetic traits common to the isolates in their respective branches of the GAS phyogenetic tree. Isogenic mutant strain MGAS315Δ*mtsR* was generated from wild-type strain MGAS315 by deleting the *mtsR* gene, using a gene replacement method described previously (4). Briefly, the upstream and downstream flanking fragments of *mtsR* were amplified by PCR using primers mtsRF1P1 and mtsRF1P2 plus mtsRF2P1 and mtsRF2P2. The gene fragments were cloned into pGRV and introduced into strain MGAS315 by electroporation to yield strain MGAS315Δ*mtsR*. Complementation of the isogenic mutant strain was accomplished by introducing a wild-type *mtsR* gene into the MGAS315Δ*mtsR* background using a standard protocol (5). The complete *mtsR* gene plus ~250 bp upstream and downstream were amplified from strain MGAS315 using primers mtsRcomp-F and mtsRcomp-R, and ligated into pCR2.1 using TOPO cloning (Invitrogen). The resulting plasmid was digested with *Kpn*I/*Nsi*I (New England Biolabs), and the *mtsR* gene segment was cloned into pDC123 (6) and introduced into MGAS315Δ*mtsR* by electroporation to yield strain MGAS315Δ*mtsR*comp. The naturally occurring *mtsR* mutant strain MGAS9887 was also complemented using this plasmid. PCR and DNA sequencing analysis showed that the correct strain constructs had been generated (Fig. S1). Southern blot analysis was performed using a probe generated with primers mtsR-seqFO and mtsR-seqRI. All oligonucleotide sequences are listed in Table S2, and the cloning strategy is described in Fig. S1.

Mouse Infection. GAS inocula were prepared by diluting freezer stocks in PBS to 10^7 cfu/mL. Immediately before inoculation, the mice were weighed and anesthetized with isoflurane (Abbott Laboratories). Five- to 6-week-old (20-25 g) outbred immunocompetent female CD1 mice (Harlan Laboratories) were used for all experiments, and they were maintained on standard laboratory food and water ad libitum. The animals were randomly assigned to treatment groups and inoculated intramuscularly in the right hindlimb with 10^6 cfu of GAS in 100 μL PBS. Several strains were studied, including MGAS315, MGAS315Δ*mtsR*, MGAS*315*Δ*mtsR*comp, and strain MGAS9887 (n = 15 animals per treatment group). Control animals were injected with PBS only. Near mortality was determined by observation every 3 h for the first 72 h, and then every 6–12 h thereafter. Mice were euthanized with isofluorane when they reached near mortality. For the quantitative culture experiment, mice were inoculated with PBS, wild-type strain MGAS315, or mutant strain MGAS315Δ*mtsR* (n = 66 animals per treatment group) and monitored every 3–6 h. The time point for the first quantitative cultures (12 h postinoculation) was selected based on observations from pilot survival experiments. The second (40 h postinoculation) and third (60 h postinoculation) time points were selected to coincide with observed near-mortality events in mice inoculated with wild-type strain MGAS315. At each time point, 22 mice per group were anesthetized, weighed, and bled via cardiac puncture. Blood was collected in 1-mL tubes containing sodium EDTA (Becton Dickinson). Mice were subsequently euthanized with isofluorane. Infected hindlimbs were surgically disarticulated and placed into preweighed tubes containing 1.5 mL of sterile PBS. The infected hindlimbs of 20 mice per group were used for quantitative culture at each time point, and two mice per group at each time point were used for correlative gross and microscopic analysis. After collection, all tissues were weighed and stored on wet ice until processed. For the myeloperoxidase assays, mice were inoculated with strain MGAS315, strain MGAS315Δ*mtsR*, or PBS (n = 9 animals per treatment group) and monitored every 6 h for near mortality. Three animals were killed at each time point as described. All mouse experimental protocols were approved by the Institutional Animal Care and Use Committee of the Methodist Hospital Research Institute.

Gross and Microscopic Pathological Analyses. Infected disarticulated mouse limbs were visually examined at 0, 6, 12, 24, 40, 48, 60, 72, and 96 h postinoculation, and representative specimens were photographed. Each limb was photographed from multiple angles to fully document all gross pathology findings. The image showing the muscle pathology characteristic of each strain was selected for publication (Figs. 1 and 5 and Fig. S5). Tissue was fixed in 10% phosphate-buffered formalin, decalcified, serially sectioned, and embedded in paraffin using automated standard instruments. Hematoxylin- and eosin-stained and Gram's-stained sections were examined with an Olympus BX5 microscope and photographed with an Olympus DP70 camera. The micrograph of tissue taken from the inoculation site that showed muscle pathology characteristic of each strain was selected for publication (Figs. 1 and 5 and Fig. S5).

Quantitative Bacterial Culture from Infected Mouse Tissue. Limbs from the infected mice were homogenized with an OMNI homogenizer (USA Scientific Inc.). Tissue homogenates and anticoagulated blood were diluted serially in sterile PBS and plated on TSA-B. The plates were incubated for 24 h at 37°C in an atmosphere of 5% CO_2 and 20% O_2, and cfu's per gram tissue or per milliliter blood were calculated. The results of each treatment group at each time point were expressed as mean ± SEM, and statistical significance was calculated by the Wilcoxon matched pairs test (Prism 4.03; GraphPad Software Inc.). Nonparametric statistical methods were used because the data did not fit a Gaussian distribution.

Myeloperoxidase Activity Assay. MPO as a surrogate marker for PMNs and associated tissue-destructive enzymes was quantified using the Mouse Myeloperoxidase Assay Kit (Hycult Biosystems) according to the manufacturer's instructions. Briefly, the infected limbs were homogenized, diluted 1:100 in PBS, and transferred to 96-well ELISA plates. Immunoreactive MPO enzyme was measured in each tissue by extrapolation from a standard curve.

The data were expressed as mean ± SD micrograms MPO per tissue), and statistical significance was calculated with Student's *t* test (Prism 4.03; GraphPad Software Inc.).

Isolation of Human PMNs. Human PMNs were isolated from venous blood of healthy individuals as described (7). All studies were performed in accordance with a protocol approved by the Institutional Review Board for Human Subjects, National Institute of Allergy and Infectious Diseases. Purified PMNs were suspended in RPMI 1640 (Invitrogen) medium buffered with 10 mM Hepes (pH 7.2; RPMI/H) and chilled on ice until used.

Bactericidal Activity Assays. Killing of GAS by human PMNs was determined as described previously with slight modification (8). PMNs (10^6) were combined with 10^7 unopsonized GAS in 96-well tissue culture plates on ice. Plates were centrifuged at 380 × *g* for 5 min and then incubated at 37 °C for 30 or 60 min. Neutrophils were lysed with 0.1% saponin for 15 min on ice, and GAS were plated on Todd–Hewitt agar containing 0.2% yeast extract. Colonies were enumerated the following day, and percent GAS survival was calculated as $(CFU_{PMN+}/CFU_{PMN-}) \times 100$. The assay measures total number of viable ingested and uningested bacteria.

To test for differential susceptibility of MGAS315 and MGAS315Δ*mtsR* to H_2O_2, strains ($1–2 \times 10^8$) were cultured to exponential (2.5 h, OD_{600} = 0.350) or stationary (7.5–8 h, OD_{600} = ~1.0) phases of growth, transferred to 1.5-mL tubes, and rotated at 37 °C with varied concentrations of H_2O_2 for 60 min. Bacteria were plated on THY agar, and colonies were enumerated the following day. Percent GAS survival was determined using the equation $(CFU_{+\text{hydrogen peroxide}}/CFU_{\text{control}}) \times 100$.

In Vitro Expression Microarray Analysis. Expression microarray analysis was performed on strain MGAS315 and MGAS315Δ*mtsR* by procedures described previously (9). Briefly, bacteria were grown in triplicate in THY medium and harvested during the exponential growth phase and at the transition from exponential to stationary phase. Transcripts were analyzed using a custom Affymetrix chip (10).

TaqMan Analysis. TaqMan real-time quantitative reverse transcription PCR (QRT-PCR) was performed in quadruplicate with an ABI Thermocycler 7700 using the ΔC_T method of analysis (Applied Biosystems). Strains were grown to mid- and late-logarithmic growth phases in THY. RNA was isolated with a FastPrep Blue Kit (MP Biochemicals) and purified using QiaShredder and RNeasy kits (Qiagen). The concentration and quality of RNA were assessed with an Agilent 2100 Bioanalyzer and analysis of the A260/A280 ratio. cDNA was created from the RNA using SuperScript III (Invitrogen) according to the manufacturer's instructions. TaqMan primers and probes for *mtsR*, *prsA*, *speB*, and the internal control gene *gyrA* are listed in Table S2.

Extracellular Caseinolytic Activity. GAS secreted protease activity was assessed by milk-plate hydrolysis, an assay specific for SpeB activity (11, 12). Briefly, 18-h GAS cultures grown in THY media were inoculated into THY-based plates composed of 2.5% nonfat milk (BioRad) and 1.25% agarose (Difco) using a 22-gauge hollow needle. The plates were incubated anaerobically for 48 h. The average diameter of proteolytic activty was determined by measuring the diameter of clearing around colonies using calipers. The data were expressed as mean diameter ± SD (mm milk clearing), and statistical significance was calculated with Student's *t* test (Prism 4.03; GraphPad Software Inc.).

In Vivo SpeB Protease Activity. SpeB protease activity was assessed by zymogen cleavage, an assay specific for SpeB activity (13). Briefly, infected monkey muscle was homogenized, clarified by centrifugation, sterile filtered, and incubated at 37 °C for 12 h in the presence of purified recombinant Cys192Ser SpeB zymogen. This mutant SpeB zymogen (40 kDa) lacks enzymatic activity, so it is unable to autocatalytically process itself into the mature enzyme (28 kDa); however, in the presence of enzymatically active SpeB, it can be fully processed. Reaction products were resolved by SDS/PAGE and immunostained with either a polyclonal anti-SpeB or monoclonal anti-HIS6× antibody (Invitrogen). Detection of the 28-kDa band following incubation of the inactive zymogen with the infected muscle homogenate confirms the presence of enzymatically active SpeB in the tissue specimen. SpeB harvested from the culture supernatant of serotype M1 strain MGAS2221 was used as a positive control, and PBS sham infected monkey muscle was used as a negative control.

Monkey Infection. The study protocol was approved by the Animal Care and Use Committee at the University of Houston. Adult male cynomolgus macaques (*Macaca fasicularis*) (Charles River BRF) ages 3–5 years were used for all experiments. All animals were housed individually and provided food and water ad libitum. Inocula of wild-type strain MGAS315 and isogenic mutant strain MGAS315Δ*mtsR* were prepared as described previously. Differences in animal weight and age were minimized during assignment to experimental groups. In the first experiment, four animals each received the wild-type strain, *mtsR* mutant strain, or PBS sham inoculation. In the second experiment, three animals each received the wild-type strain, *prsA*-overexpressing strain, or *speB* inactivated strain. For experimental infections, each animal was inoculated with 1.0×10^8 cfu/kg in 500 μL PBS. Each animal was anesthetized (see next section), outfitted with a nylon mesh jacket overlying a transdermal fentanyl patch, and inoculated intramuscularly in the anterior thigh to a uniform depth. The animals were observed continuously and killed when they were judged to be near death.

Monkey Anesthesia and Sedation. The animals were sedated with tiletamine HCl and zolazepam HCl (Fort Dodge Animal Health) at a dose of 2 mg/kg intramuscularly. They were clipped with a no. 40 blade over the thorax, and a 25 μg/h fentanyl patch was sutured in place over the shaved area (Sandoz). A mesh jacket (Lomir Biomedical, Inc.) was fitted to each monkey to protect the fentanyl patch. All animals were acclimatized to the jackets 2 weeks before the start of the study. Each animal was inoculated intramuscularly in the anterior thigh at a uniform depth. Subsequent sedations were done with either a combination of tiletamine HCl and zolazepam HCl (Telazol; Fort Dodge Animal Health) at a dose of 2 mg/kg intramuscularly or ketamine HCl (Vedco) at a dose of 7–15 mg/kg intramuscularly. Animals were observed continuously for the first 48 h and every 2 h for the next 24 h. Animals were euthanized in matched pairs when they were determined to be moribund.

Creatine Kinase Assays. The level of creatine kinase in serum obtained from monkeys at sacrifice was measured by automated enzymatic analysis using a coupled Oliver–Rosalki method on a Beckman CX7 analyzer (Equine Laboratories).

Determination of Monkey Muscle Lesion Area. Lesion size in the infected monkeys was determined immediately following sacrifice. The margin of viable/nonviable muscle was identified by visual inspection of overt necrosis, abscess formation, dusky discoloration, erythema, and edema. The diameter of the lesion in the greatest dimension (major axis) and its two perpendicular line segments (minor axes) were measured with a caliper and applied to the formula for calculating the volume of a scalene ellipse.

1. Beres SB, et al. (2006) Molecular genetic anatomy of inter- and intraserotype variation in the human bacterial pathogen group A *Streptococcus*. *Proc Natl Acad Sci USA* 103:7059–7064.
2. Beres SB, et al. (2002) Genome sequence of a serotype M3 strain of group A *Streptococcus*: Phage-encoded toxins, the high-virulence phenotype, and clone emergence. *Proc Natl Acad Sci USA* 99:10078–10083.
3. Beres SB, et al. (2004) Genome-wide molecular dissection of serotype M3 group A *Streptococcus* strains causing two epidemics of invasive infections. *Proc Natl Acad Sci USA* 101:11833–11838.
4. Hanks TS, et al. (2006) Differential regulation of iron- and manganese-specific MtsABC and heme-specific HtsABC transporters by the metalloregulator MtsR of group A *Streptococcus*. *Infect Immun* 74:5132–5139.
5. Shelburne SA, 3rd, et al. (2006) Maltodextrin utilization plays a key role in the ability of group A *Streptococcus* to colonize the oropharynx. *Infect Immun* 74:4605–4614.
6. Chaffin DO, Rubens CE (1998) Blue/white screening of recombinant plasmids in Gram-positive bacteria by interruption of alkaline phosphatase gene (phoZ) expression. *Gene* 219:91–99.
7. Kobayashi SD, et al. (2003) Bacterial pathogens modulate an apoptosis differentiation program in human neutrophils. *Proc Natl Acad Sci USA* 100:10948–10953.
8. Hoe NP, et al. (2002) Insight into the molecular basis of pathogen abundance: Group A *Streptococcus* inhibitor of complement inhibits bacterial adherence and internalization into human cells. *Proc Natl Acad Sci USA* 99:7646–7651.
9. Sitkiewicz I, et al. (2006) Emergence of a bacterial clone with enhanced virulence by acquisition of a phage encoding a secreted phospholipase A2. *Proc Natl Acad Sci USA* 103:16009–16014.
10. Virtaneva K, et al. (2005) Longitudinal analysis of the group A *Streptococcus* transcriptome in experimental pharyngitis in cynomolgus macaques. *Proc Natl Acad Sci USA* 102: 9014–9019.
11. Chaussee MS, Ajdic D, Ferretti JJ (1999) The *rgg* gene of *Streptococcus pyogenes* NZ131 positively influences extracellular SPE B production. *Infect Immun* 67: 1715–1722.
12. Reid SD, et al. (2006) Inactivation of the group A *Streptococcus* regulator srv results in chromosome wide reduction of transcript levels, and changes in extracellular levels of Sic and SpeB. *FEMS Immunol Med Microbiol* 48:283–292.
13. Doran JD, et al. (1999) Autocatalytic processing of the streptococcal cystein protease zymogen: Processing mechanism and characterization of the autoproteolytic cleavage sites. *Eur J Biochem* 263:145–151.

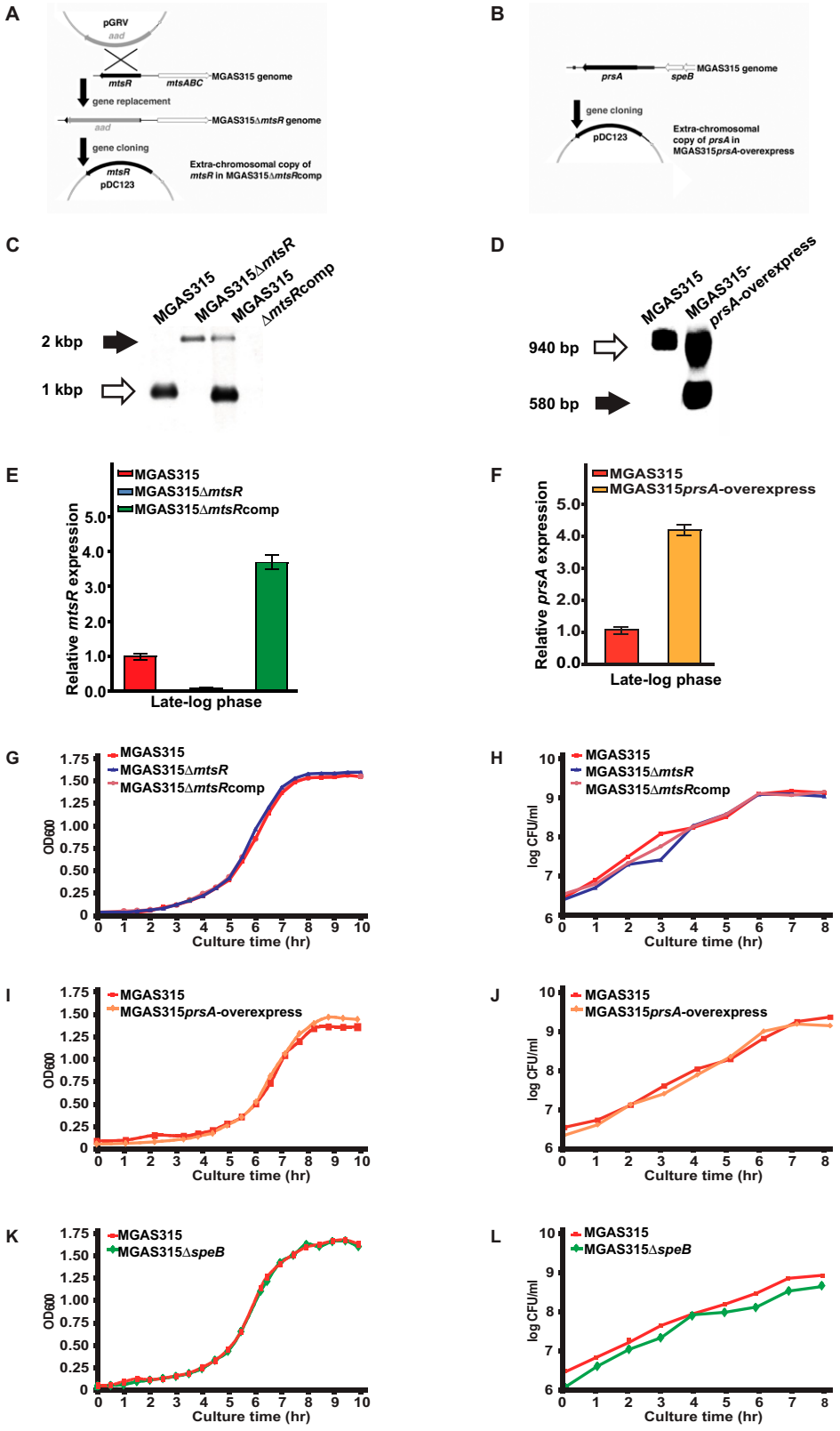

Fig. S1. Construction and confirmation of isogenic strains MGAS315Δ*mtsR*, MAS315Δ*mtsR*comp, MGAS315*prsA*-overexpress, and MGAS315Δ*speB*. (*A*) Molecular genetic strategy for inactivating *mtsR* in strain MGAS315. The *mtsR* gene in strain MGAS315 was replaced with the *aad* gene conferring spectinomycin resistance to generate the isogenic mutant strain MGAS315Δ*mtsR*. Strain MGAS315Δ*mtsR* was complemented with an extrachromosomal copy of *mtsR* cloned into pDC123 to generate strain MGAS315Δ*mtsR*comp. (*B*) Strain MGAS315*prsA*-overexpress was generated by providing MGAS315 with an extrachromosomal copy of *prsA* cloned into pDC123. All primers and probes are listed in Table S2. (*C*) Southern blot showing the intact *mtsR* gene (white arrow) in wild-type strain MGAS315 and the deleted *mtsR* gene (black arrow) in mutant strain MGAS315Δ*mtsR*. Strain MGAS315Δ*mtsR*comp has both the deleted genomic copy of the *mtsR* gene (black arrow) and the complemented extrachromosomal *mtsR* gene (white arrow). (*D*) Southern blot showing the intact *prsA* gene (white arrow) in

strain MGAS315. Strain MGAS315*prsA*-overexpress has both the genomic copy of the *prsA* gene (white arrow) and the extrachromosomal *prsA* gene (black arrow). (*E*) TaqMan quantitative PCR confirmed that compared with wild-type strain MGAS315, the isogenic mutant strain MGAS315Δ*mtsR* does not express *mtsR* transcript. Genetic complementation to create strain MGAS315Δ*mtsR*comp restores *mtsR* expression. (*F*) TaqMan quantitative PCR confirmed that compared with wild-type strain MGAS315, strain MGAS315*prsA*-overexpress overexpresses *prsA* transcript. (*G*) Growth curves of wild-type (MGAS315), *mtsR* isogenic mutant (MGAS315Δ*mtsR*), and complemented mutant (MGAS315Δ*mtsR*comp*)* GAS strains grown in THY. OD_{600} readings were taken at indicated times for growth in THY medium. (*H*) Growth curves strains MGAS315, MGAS315Δ*mtsR*, and MGAS315Δ*mtsR*comp with quantitative cfu's performed. (*I*) Growth curves of wild-type (MGAS315) and *prsA*-overexpressing (MGAS315*prsA*-overexpress) GAS strains. (*J*) Growth curves of MGAS315 and MGAS315*prsA*-overexpress with quantitative cfu's performed. (*K*) Growth curves of wild-type (MGAS315) and *speB* isogenic mutant (MGAS315Δ*speB*) GAS strains. (*L*) Growth curves of strains MGAS315 and MGAS315Δ*speB* with quantitative cfu's performed. Inactivation of *mtsR*, overexpression of *prsA,* or inactivation of *speB* had no significant effect on GAS growth in vitro in nutrient rich media.

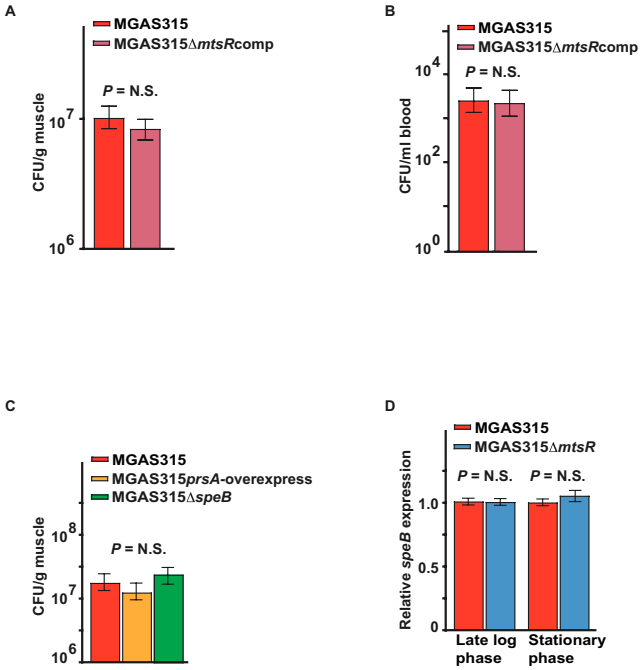

Fig. S2. (*A*) Quantitative culture of muscle from mice infected with wild-type strain MGAS315 or gene complemented mutant strain MGAS315Δ*mtsR*comp. (*B*) Quantitative culture of blood from mice infected with strains MGAS315 or MGAS315Δ*mtsR*comp. (*C*) Quantitative culture of muscle from mice infected with wild-type strain MGAS315 or isogenic mutant strains MGAS315*prsA*-overexpress and MGAS315Δ*speB.* (*D*) TaqMan analysis of *speB* transcript level in strain MGAS315 or MGAS315Δ*mts.*

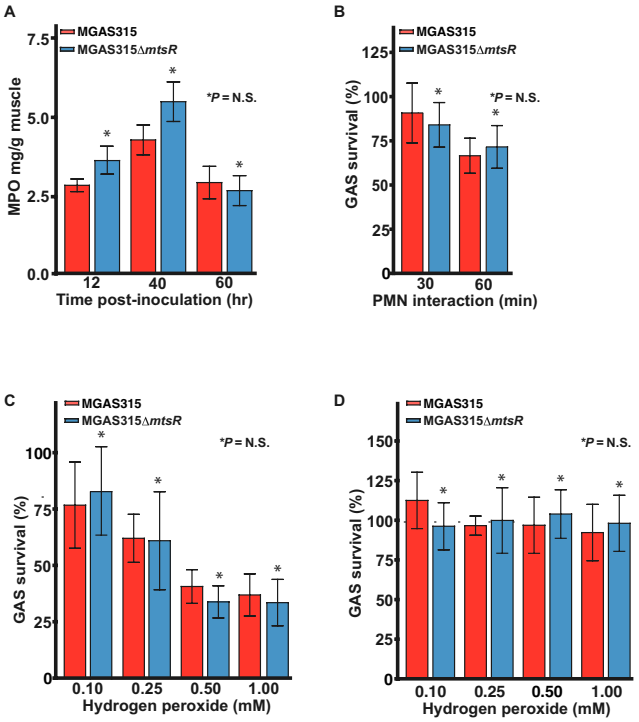

Fig. S3. Inactivation of *mtsR* has no significant effect on GAS recruitment of host PMNs or survival after human PMN phagocytosis and exposure to hydrogen peroxide. (*A*) Level of immunoreactive myeloperoxidase (MPO) in limb tissue homogenates. Mice were inoculated intramuscularly in the hindlimb with wild-type strain MGAS315 or isogenic mutant strain MGAS315Δ*mtsR* (n = 9 animals per treatment group). The mice were killed at each time point, infected limbs were homogenized, and MPO levels in the homogenates were determined using a commercially available antigen-capture assay. There was no significant difference in immunoreactive MPO present in the mouse groups at any of the time points. (*B*) PMN bactericidal activity. Human PMNs were cultured with MGAS315 or MGAS315Δ*mtsR* for the indicated times, and killing of bacteria was determined. There was no significant difference in survival at either time point. (*C* and *D*) Killing of GAS by H_2O_2. GAS were cultured to midexponential (*C*) or stationary phase (*D*) of growth and incubated for 60 min with H_2O_2.

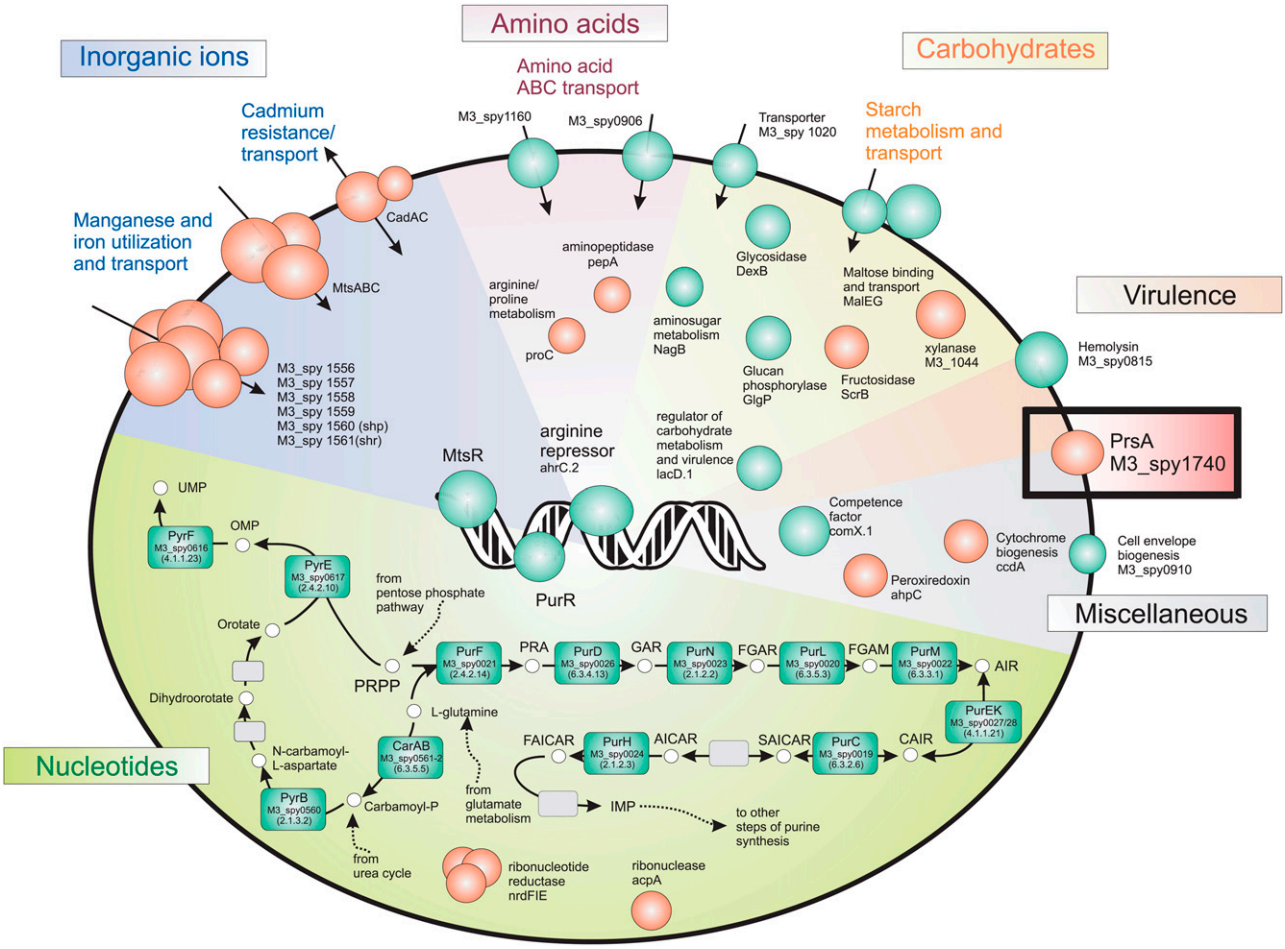

Fig. S4. Schematic summarizing significant differences in gene transcript level between wild-type strain MGAS315 and isogenic mutant strain MGAS315Δ*mtsR*. Red circles and rectangles denote transcripts significantly increased in the mutant strain relative to the wild-type strain, whereas green circles and rectangles represent transcripts that are significantly decreased in the mutant strain. The up-regulated *prsA* transcript is identified by the rectangle on the right side of the figure. Gene numbers refer to gene annotations (Table S1).

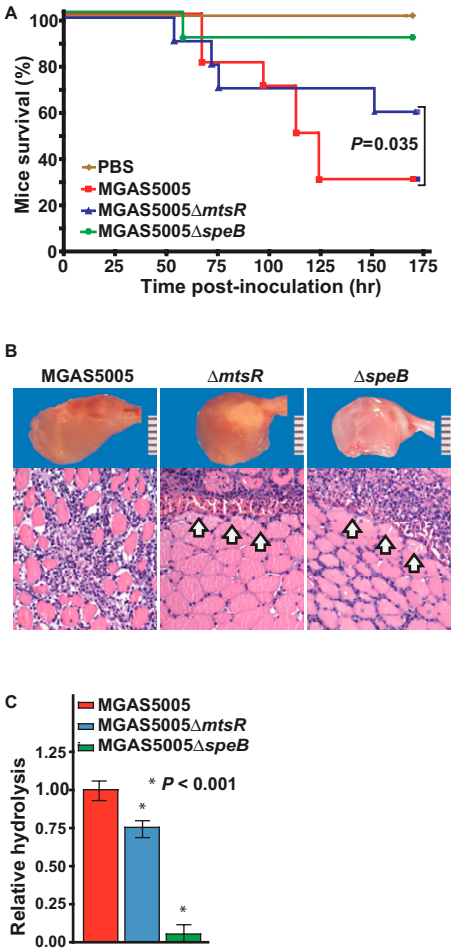

Fig. S5. (*A*) Kaplan–Meier survival curves for mice inoculated intramuscularly with a panel of isogenic serotype M1 strain GAS organisms MGAS5005, MGAS5005Δ*mtsR*, or MGAS5005Δ*speB*. (*B*) Visual and microscopic examination of mice inoculated intramuscularly with isogenic serotype M1 strain GAS organisms. Wild-type strain MGAS5005 caused diffuse soft tissue necrosis, whereas strains MGAS5005Δ*mtsR* and MGAS5005Δ*speB* caused significantly less necrotic lesions that were confined to the inoculation site (arrows). These pathologic features are similar to those observed in mice inoculated with the serotype M3 strains (see Fig. 1). (*C*) Milk agar assay for SpeB activity. Compared with the wild-type, strains MGAS5005Δ*mtsR* and MGAS5005Δ*speB* have significantly less proteolytic activity.

Table S1. Ratios of Δ*mtsR*/wild type in exponential and transition from exponential to stationary phase

SF370 ORF number	MGAS315 ORF	Gene	Abundance in mtsR mutant (EXP)	Abundance in mtsR mutant (EXP/S)	Functional Category	Functional Sub-category	Putative function
Spy0112	SpyM3_0088	proC		1.72	Metabolism	Amino acid transport and metabolism	Pyrroline-5-carboxylate reductase
Spy0833	SpyM3_0561	carA		0.57	Metabolism	Amino acid transport and metabolism	Carbamoylphosphate synthase small subunit
Spy0835	SpyM3_0562	carB		0.55	Metabolism	Amino acid transport and metabolism	Carbamoylphosphate synthase large subunit (split gene in MJ)
Spy1274	SpyM3_0906			0.61	Metabolism	Amino acid transport and metabolism	ABC-type amino acid transport/signal transduction systems, periplasmic component/domain
Spy1506	SpyM3_1160	-		0.59	Metabolism	Amino acid transport and metabolism	ABC-type polar amino acid transport system, ATPase component
Spy1549	SpyM3_1198	ahrC.2		0.66	Metabolism	Amino acid transport and metabolism	Arginine repressor
Spy0115	SpyM3_0089	pepA	1.59	1.76	Metabolism	Carbohydrate transport and metabolism	Cellulase M and related proteins
Spy1291	SpyM3_0980	glgP		0.48	Metabolism	Carbohydrate transport and metabolism	Glucan phosphorylase
Spy1294	SpyM3_0983	malE		0.51	Metabolism	Carbohydrate transport and metabolism	Maltose-binding periplasmic proteins/domains
Spy1296	SpyM3_0985	malG		0.46	Metabolism	Carbohydrate transport and metabolism	ABC-type maltose transport systems, permease component
Spy1340	SpyM3_1020	-	0.62	0.48	Metabolism	Carbohydrate transport and metabolism	Permeases of the major facilitator superfamily
Spy1399	SpyM3_1065	nagB		0.61	Metabolism	Carbohydrate transport and metabolism	6-phosphogluconolactonase/Glucosamine-6-phosphate isomerase/deaminase
Spy1704	SpyM3_1482	lacD.1		0.64	Metabolism	Carbohydrate transport and metabolism	Tagatose-1,6-bisphosphate aldolase
SPy1973	SpyM3_1695	dexB		0.65	Metabolism	Carbohydrate transport and metabolism	Glycosidases
Spy1370	SpyM3_1044	-	2.98	2.04	Metabolism	Carbohydrate transport and metabolism	Predicted xylanase/chitin deacetylase
Spy1816	SpyM3_1570	scrB		1.50	Metabolism	Carbohydrate transport and metabolism	Beta-fructosidases (levanase/invertase)
Spy1280	SpyM3_0910	glmS	0.65	0.57	Cellular processes and signaling	Cell wall/membrane/envelope biogenesis	Glucosamine 6-phosphate synthetase, contains amidotransferase and phosphosugar isomerase domains
Spy0814	SpyM3_0547	folC.2		1.59	Metabolism	Coenzyme transport and metabolism	Folylpolyglutamate synthase
Spy1790	SpyM3_1556	-		1.78	Cellular processes and signaling	Defense mechanisms	ABC-type multidrug transport system, ATPase and permease components
Spy0148	SpyM3_0115	ntpI		0.62	Metabolism	Energy production and conversion	Archaeal/vacuolar-type H+-ATPase subunit I
Spy1128	SpyM3_0787	pta		0.64	Metabolism	Energy production and conversion	Phosphotransacetylase
Spy1791	SpyM3_1557	-	1.79	4.00	Metabolism	Energy production and conversion	ABC-type transport system involved in cytochrome bd biosynthesis, ATPase and permease components
Spy1113	SpyM3_0773	-		0.54	Hypothetical	General function predicted	Acid phosphatase (class B)
Spy1325	SpyM3_1005	-		0.58	Hypothetical	General function predicted	putative transcriptional antiterminator
Spy2162	SpyM3_1818	cadD		0.66	Metabolism	Inorganic ion transport and metabolism	Predicted permease, cadmium resistance protein
Spy0453	SpyM3_0318	mtsA	2.72		Metabolism	Inorganic ion transport and metabolism	ABC-type Mn/Zn transport system, periplasmic Mn/Zn-binding (lipo)protein (surface adhesin A)
Spy0454	SpyM3_0319	mtsB	3.04		Metabolism	Inorganic ion transport and metabolism	ABC-type Mn/Zn transport systems, ATPase component

Table S1. Cont.

Spy0456	SpyM3_0320	mtsC	**3.08**		Metabolism	Inorganic ion transport and metabolism	ABC-type Mn2+/Zn2+ transport systems, permease components
SPy1434	SpyM3_1093	cadA	**2.63**	**2.87**	Metabolism	Inorganic ion transport and metabolism	Cation transport ATPases
Spy1793	SpyM3_1558	-	**2.43**	**4.87**	Metabolism	Inorganic ion transport and metabolism	ABC-type cobalamin/Fe3+-siderophores transport systems, ATPase components
Spy1794	SpyM3_1559	-	**2.08**	**4.87**	Metabolism	Inorganic ion transport and metabolism	ABC-type Fe3+-siderophore transport system, permease component
Spy1795	SpyM3_1560	shp	**1.89**	**4.39**	Metabolism	Inorganic ion transport and metabolism	ABC-type Fe3+-hydroxamate transport system, periplasmic component
Spy1798	SpyM3_1561	shr	**3.21**	**8.06**	Metabolism	Inorganic ion transport and metabolism	Putative Fe3+-siderophore transport protein
Spy0140	SpyM3_0108			**0.62**	Metabolism	Lipid transport and metabolism	Acetyl-CoA acetyltransferase
SPy0025	SpyM3_0020	-	**0.63**		Metabolism	Nucleotide transport and metabolism	Phosphoribosylformylglycinamidine (FGAM) synthase, synthetase domain
Spy0026	SpyM3_0021	purF		**0.54**	Metabolism	Nucleotide transport and metabolism	Glutamine phosphoribosylpyrophosphate amidotransferase
not annotated	SpyM3_0024	-	**0.63**		Metabolism	Nucleotide transport and metabolism	AICAR transformylase/IMP cyclohydrolase PurH (only IMP cyclohydrolase domain in Aful)
Spy0033	SpyM3_0027	purE		**0.66**	Metabolism	Nucleotide transport and metabolism	Phosphoribosylcarboxyaminoimidazole (NCAIR) mutase
Spy0425	SpyM3_0301	nrdF.1	**18.61**	**5.49**	Metabolism	Nucleotide transport and metabolism	Ribonucleotide reductase beta subunit
Spy0426	SpyM3_0302	nrdI	**27.07**	**10.10**	Metabolism	Nucleotide transport and metabolism	Protein involved in ribonucleotide reduction
Spy0427	SpyM3_0303	nrdE.1	**30.63**	**10.31**	Metabolism	Nucleotide transport and metabolism	Ribonucleotide reductase alpha subunit
Spy0831	SpyM3_0559	pyrP		**0.56**	Metabolism	Nucleotide transport and metabolism	Xanthine/uracil permeases
Spy0832	SpyM3_0560	pyrB		**0.55**	Metabolism	Nucleotide transport and metabolism	Aspartate carbamoyltransferase, catalytic chain
Spy0872	SpyM3_0591	-	**0.62**	**0.58**	Metabolism	Nucleotide transport and metabolism	5'-nucleotidase/2',3'-cyclic phosphodiesterase and related esterases
Spy0900	SpyM3_0616	pyrF		**0.38**	Metabolism	Nucleotide transport and metabolism	Orotidine-5'-phosphate decarboxylase
Spy0901	SpyM3_0617	pyrE		**0.50**	Metabolism	Nucleotide transport and metabolism	Orotate phosphoribosyltransferase
Spy1163	SpyM3_0794	xpt	**0.55**		Metabolism	Nucleotide transport and metabolism	Adenine/guanine phosphoribosyltransferases and related PRPP-binding proteins
not present	SpyM3_0686			**1.75**	Mobile genetic element	Phage	Transcriptional regulator
not present	SpyM3_0690			**1.98**	Mobile genetic element	Phage	Replicative DNA helicase
not present	SpyM3_0692			**1.79**	Mobile genetic element	Phage	Archaeal/vacuolar-type H+-ATPase subunit A
not annotated	SpyM3_0694			**1.64**	Mobile genetic element	Phage	
not present	SpyM3_0696			**1.94**	Mobile genetic element	phage	
not present	SpyM3_0701		**2.43**		Mobile genetic element	Phage	Transcriptional regulator
not present	SpyM3_0732			**0.49**	Mobile genetic element	phage	
not present	SpyM3_0734			**0.57**	Mobile genetic element	Phage	
not present	SpyM3_0736		**0.60**	**0.50**	Mobile genetic element	Phage	Predicted transcriptional regulators
SPy0701	SpyM3_0928			**1.87**	Mobile genetic element	Phage	
not present	SpyM3_0952		**1.92**		Mobile genetic element	Phage	
not present	SpyM3_0953		**1.81**		Mobile genetic element	Phage	SAM-dependent methyltransferases
not present	SpyM3_0956		**1.84**		Mobile genetic element	Phage	

Table S1. Cont.

not present	SpyM3_0959		**1.68**		Mobile genetic element	Phage	
not present	SpyM3_0961		**1.53**		Mobile genetic element	Phage	Phage DNA/RNA helicase (DEAD/DEAH box family)
not present	SpyM3_0962		**1.81**		Mobile genetic element	Phage	
not present	SpyM3_0964		**1.70**		Mobile genetic element	Phage	Predicted transcriptional regulators
not present	SpyM3_0965		**2.14**		Mobile genetic element	Phage	
not present	SpyM3_0966		**2.31**		Mobile genetic element	Phage	
not present	SpyM3_0968			**0.40**	Mobile genetic element	Phage	
not present	SpyM3_0969			**0.43**	Mobile genetic element	Phage	
not present	SpyM3_0970		**2.66**		Mobile genetic element	Phage	
not present	SpyM3_0971		**1.67**		Mobile genetic element	Phage	Predicted transcriptional regulators
not present	SpyM3_0978	int.1		**0.55**	Mobile genetic element	Phage	Integrase
Spy0681	SpyM3_1231			**3.20**	Mobile genetic element	Phage	
not present	SpyM3_1235			**2.87**	Mobile genetic element	Phage	
not present	SpyM3_1246			**1.54**	Mobile genetic element	Phage	
not present	SpyM3_1259			**0.56**	Mobile genetic element	Phage	
Spy0977	SpyM3_1324			**1.94**	Mobile genetic element	Phage	
	SpyM3_1354			**0.59**	Mobile genetic element	phage	
not present	SpyM3_1420			**1.79**	Mobile genetic element	phage	
not present	SpyM3_1422			**1.49**	Mobile genetic element	phage	
not present	SpyM3_1423			**1.58**	Mobile genetic element	phage	
not present	SpyM3_1424			**1.84**	Mobile genetic element	phage	
not present	SpyM3_1425			**1.62**	Mobile genetic element	phage	
not present	SpyM3_1426			**1.99**	Mobile genetic element	phage	
not present	SpyM3_1427			**1.74**	Mobile genetic element	phage	
not present	SpyM3_1428	-	**1.65**	**1.77**	Mobile genetic element	Phage	
not present	SpyM3_1429			**1.78**	Mobile genetic element	phage	
not present	SpyM3_1430			**2.00**	Mobile genetic element	phage	
Spy0685	SpyM3_1431			**1.88**	Mobile genetic element	Phage	
not present	SpyM3_1435			**1.62**	Mobile genetic element	phage	
not present	SpyM3_1437	-		**1.54**	Mobile genetic element	Phage	
not present	SpyM3_1438			**1.46**	Mobile genetic element	Phage	
not present	SpyM3_1446	-	**1.84**	**1.66**	Mobile genetic element	Phage	
not present	SpyM3_1450		**1.92**	**1.70**	Mobile genetic element	Phage	

Table S1. Cont.

not present	SpyM3_1453		**1.50**		Mobile genetic element	Phage	
not annotated (SpyM18_1620)	not annotated			**0.63**	Hypothetical	Poorly characterized	
Spy0116	not annotated			**4.69**	Hypothetical	Poorly characterized	
Spy0100	SpyM3_0077	-		**0.61**	Hypothetical	Poorly characterized	putative DNA binding protein
Spy0205	SpyM3_0150	-		**0.57**	Hypothetical	Poorly characterized	
Spy0470	SpyM3_0332	-		**1.59**	Hypothetical	Poorly characterized	Myosin-crossreactive antigen
Spy0519	SpyM3_0367	-		**0.64**	Hypothetical	Poorly characterized	ABC-type uncharacterized transport system, permease component
Spy0617	SpyM3_0436			**1.53**	Hypothetical	Poorly characterized	Predicted hydrolases of the HAD superfamily
Spy0843	SpyM3_0569	-	**1.96**	**1.92**	Hypothetical	Poorly characterized	Predicted flavin-nucleotide-binding protein structurally related to pyridoxine 5'-phosphate oxidase
Spy0844	SpyM3_0570	-	**1.89**	**1.90**	Hypothetical	Poorly characterized	Predicted flavin-nucleotide-binding protein structurally related to pyridoxine 5'-phosphate oxidase
Spy0914	SpyM3_0629			**0.61**	Hypothetical	Poorly characterized	
Spy0915	SpyM3_0630			**0.65**	Hypothetical	Poorly characterized	Predicted sulfurtransferase
not annotated	SpyM3_1092	-	**1.73**	**1.76**	Hypothetical	Poorly characterized	
Spy1581	SpyM3_1282	-		**1.51**	Hypothetical	Poorly characterized	Uncharacterized conserved protein, contains double-stranded beta-helix domain
Spy1607	SpyM3_1355			**0.64**	Hypothetical	Poorly characterized	
Spy1691	SpyM3_1473	-		**0.65**	Hypothetical	Poorly characterized	
Spy1736	SpyM3_1509	-		**0.59**	Hypothetical	Poorly characterized	Permeases
SPy0219	SpyM3_1705		**0.21**		Hypothetical	Poorly characterized	Protein involved in ribonucleotide reduction
Spy2107	SpyM3_1793	-		**0.57**	Hypothetical	Poorly characterized	Predicted dehydrogenases and related proteins
Spy2173	SpyM3_1829			**1.82**	Hypothetical	Poorly characterized	Predicted membrane protein
Spy2174	SpyM3_1830			**2.41**	Hypothetical	Poorly characterized	
Spy0379	SpyM3_0277	pflC		**0.65**	Cellular processes and signaling	Posttranslational modification, protein turnover, chaperones	Pyruvate-formate lyase-activating enzyme
Spy0888	SpyM3_0607	clpL		**0.50**	Cellular processes and signaling	Posttranslational modification, protein turnover, chaperones	ATPases with chaperone activity, ATP-binding subunit
Spy0917	SpyM3_0631	-	**0.44**		Cellular processes and signaling	Posttranslational modification, protein turnover, chaperones	Glutathione S-transferase
SPy1559	SpyM3_1269	ccdA		**1.67**	Cellular processes and signaling	Posttranslational modification, protein turnover, chaperones	Cytochrome c biogenesis protein
Spy2079	SpyM3_1770	ahpC		**1.68**	Cellular processes and signaling	Posttranslational modification, protein turnover, chaperones	Peroxiredoxin
Spy1196	SpyM3_0839	-		**0.54**	Information storage and processing	Replication, recombination and repair	
Spy1785	SpyM3_1551	recG		**1.81**	Information storage and processing	Replication, recombination and repair	RecG-like helicase
Spy0471	SpyM3_0333	phoH		**1.47**	Cellular processes and signaling	Signal transduction mechanisms	Phosphate starvation-inducible protein PhoH, predicted ATPase
Spy0216	SpyM3_0157	-		**0.58**	Information storage and processing	Transcription	Transcriptional regulator
Spy0300	SpyM3_0220	comX1.1	**0.03**	**0.04**	Information storage and processing	Transcription	Competence-specific factor

Table S1. Cont.

Spy0450	SpyM3_0317	mtsR	**0.00**	**0.01**	Information storage and processing	Transcription	Mn-dependent transcriptional regulator
Spy0531	SpyM3_0375	acpA		**1.47**	Information storage and processing	Transcription	dsRNA-specific ribonuclease
Spy0830	SpyM3_0558	pyrR		**0.58**	Information storage and processing	Transcription	putative transcriptional regulator
Spy2172	SpyM3_1828			**2.28**	Information storage and processing	Transcription	Predicted transcriptional regulators
Spy0250	SpyM3_0178	rpmH		**0.39**	Information storage and processing	Translation, ribosomal structure and biogenesis	
Spy0902	SpyM3_0618	amiC		**0.64**	Information storage and processing	Translation, ribosomal structure and biogenesis	Asp-tRNAAsn/Glu-tRNAGln amidotransferase A subunit and related amidases
Spy1232	SpyM3_0870			**0.54**	Information storage and processing	Translation, ribosomal structure and biogenesis	16S RNA G1207 methylase RsmC
Spy1689	SpyM3_1472	glyQ		**1.64**	Information storage and processing	Translation, ribosomal structure and biogenesis	Glycyl-tRNA synthetase, alpha subunit
Spy1888	SpyM3_1629	rpmB		**0.65**	Information storage and processing	Translation, ribosomal structure and biogenesis	Ribosomal protein L28
Spy0303	SpyM3_0221	-	**0.18**		Mobile genetic element	Transposase	
Spy0116	SpyM3_1015		**6.61**		Mobile genetic element	Transposase	
SPy0303	SpyM3_1704	-	**0.20**	**0.57**	Mobile genetic element	Transposase	
Spy1159	SpyM3_0815	-	**0.63**		Virulence	Virulence	Predicted membrane protein, hemolysin III homolog
SPy2037	SpyM3_1740	prsA	**1.81**		Virulence	Virulence	Protein export protein prsA precursor

Table S2. Primers and probes used in analysis

Primer	Sequence	Application
mtsR-F1P1	AACTGCAGCTTTGCAATCAATTGTTTGGC	Upstream fragment of *mtsR* for *mtsR* deletion
mtsR-F1P2	GAAGATCTGTAATCTTCTTTATTAGGCGTC	
mtsR-F2P1	CGGGATCCGGCGACAAGGAACTTGTCATC	Downstream fragment of *mtsR* for *mtsR* deletion
mtsR-F2P2	AGTGTCGACTTCGGCCCAGACATTAATGAC	
mtsRcomp-F	GTGCCAGTTGACGAACAAGC	Ligation of *mtsR* gene into pTOPO; sequencing of *mtsR*
mtsRcomp-R	GCCCACACGGAGGGACTATT	
mtsR-seqF	CGGCTACCAAGATGACCTAG	Sequencing and PCR confirmation of *mtsR*
mtsR-seqR	CGTGATGGTGTTGAGAGTTGT	
mtsR-F-taqM3_317	GCCCACACGGAGGGACTAT	TaqMan analysis of *mtsR* gene expression
mtsR-R-taqM3_317	GATGGTGTTGAGAGTTGTAGTGTTCA	
mtsR-P-taqM3_317	CCTCGCTATGGTCAGCCTCTTGTCGA	
prsA-D	GGTATAGTCAGATTGGGTAG	Ligation of *prsA* gene into pTOPO
prsA-E	GGTCATCAACGCCTACTAATG	
pDC123-seq1	CCTTATTAACATTCACAAC	Sequencing and PCR confirmation of *mtsR* and *prsA*
pDC123-seq2	ATTCCCCATGCCATCTCCAATC	
prsA-tmF	TGGTAACGCTGGCGACAGT	TaqMan analysis of *prsA* gene expression
prsA-tmR	CGAGGTTGGTGTTGTTGTGTGA	
prsA-tmP	TGACCTTATCAGCTTGTC	
speB-5′	TGCCTACAACAGCACTTTGG	TaqMan analysis of *speB* gene expression
speB-3;	GTGGGTCTCTGACGGCTTCT	
speB-probe	GCCTGCGCCGCCACCAGTA	
gyrA F taq M3_810	CGCTGTCAAGATGGTAATGGAA	TaqMan analysis of gyrA (endogenous in vitro) gene expression
gyrA R taq M3_810	CCTGAGCGCCCCATAACA	
gyrA P taq M3_810	TCCCTGGACCTGACTTTCCGACTGG	